In vitro models (2022) 1:423–435
https://doi.org/10.1007/s44164-022-00027-8

ORIGINAL RESEARCH

Introducing CELLBLOKS®: a novel organ-on-a-chip platform allowing a plug-and-play approach towards building organotypic models

Valon Llabjani[1] · M. R. Siddique[1] · Anaïs Macos[1] · Afaf Abouzid[1] · Valmira Hoti[1] · Francis L. Martin[1] · Imran I. Patel[1] · Ahtasham Raza[1]

Received: 15 April 2022 / Revised: 15 June 2022 / Accepted: 16 June 2022 / Published online: 4 July 2022

Abstract

Human organs are structurally and functionally complex systems. Their function is driven by the interactions between many specialised cell types, which is difficult to unravel on a standard Petri dish format. Conventional "Petri dish" approaches to culturing cells are static and self-limiting. However, current organ-on-a-chip technologies are difficult to use, have a limited throughput and lack compatibility with standard workflow conditions. We developed CELLBLOKS® as a novel "plug-and-play" organ-on-a-chip platform that enables straightforward creation of multiple cell-type organ-specific microenvironments. Herein, we demonstrate its advantages by building a liver model representative of live tissue function. CELLBLOKS® allows one to systematically test and identify various cell combinations that replicate optimal hepatic relevance. The combined interactions of fibroblasts, endothelial cells and hepatocytes were analysed using hepatic biochemistry (CYP3A4 and urea), cellular proliferation indices and transporter activities (albumin). The results demonstrate that optimal liver function can be achieved by exploiting crosstalk in co-culture combinations compared to conventional mono-culture. The optimised CELLBLOKS® liver model was tested to analyse drug-induced liver toxicity using tamoxifen. The data suggests that our CELLBLOKS® liver model is highly sensitive to toxic insult compared to mono-culture liver models. In summary, CELLBLOKS® provides a novel cell culture technology for creating human-relevant organotypic models that are easy and straightforward to establish in laboratory settings.

Keywords CELLBLOKS® · Co-culture · CYP3A4 · Liver · Organ-on-a-chip platform · Tamoxifen

Introduction

In vitro models aiming to simulate real organ functions for research need to consider complex tissue microenvironments that not only includes parenchymal cells but also their interactions with surrounding cells such as endothelial cells, fibroblasts and immune cells, in addition to the extracellular matrix composites [1–3]. In drug discovery, high rates of drug attrition in clinical trials suggest there are limitations in current prediction capabilities of present preclinical models (both in vitro and in vivo models). Drug-induced liver injury (DILI) continues to be the leading cause of attrition during drug development in all phases of clinical trials as well as the number one cause of post-market drug withdrawal, accounting for 20–40% of all cases [4–6].

There is a general prerequisite that novel technologies need to be simple, rapid and physiologically relevant to the human liver, so as to provide improved predictive models for drug discovery [7, 8]. Several in vitro and in vivo models are used to screen for DILI-related toxicity issues. However, the main limitations with animal tests include the differences in physiological parameters (i.e. genetics and metabolic processes) between humans and rodents [9–11]. Out of 150 studied hepatotoxins, both rodents (primary rat) and non-rodents (e.g. canine) models only detected 50% of human hepatoxic events associated with these agents [12]. Additionally, standard in vitro models lack immune system incorporation, and there is failure to account for crosstalk with other cell types, which is important in driving their hepatic relevance [13].

In vitro approaches used to create more relevant organ-specific functions have conventionally involved either

✉ Valon Llabjani
valon@revivocell.com

[1] REVIVOCELL Limited, Sci-Tech Daresbury, Keckwick Lane, Daresbury, Warrington WA4 4AD, UK

mixing different cell types randomly, in one well, or a sandwich culture method where cell types are built in layers, consecutively, one cell type at a time. Although the sandwich approach aims to mimic tissue architecture, the method is time-consuming, difficult to reproduce and labour intensive [14]. Similarly, randomly arranged co-cultures are likely to result in a highly variably output with each experimental repeat leading to uncontrolled cell attachment, aggregation and migration that can change with different cell–cell ratios [15, 16]. Furthermore, analysis of each cell type separately is not an option in co-culture models.

Although several organ-on-chip (OoCs) microfluidic-based approaches have been recently introduced as alternatives to conventional grown cells on 2-D surfaces, these models are likely to require further comprehensive characterisation before being routinely adapted into drug discovery pipelines [8]. Their adaptation is limited because they are substantially different to conventionally used industry standard multi-well plates that have shortcomings in both handling and biological characterisations; they differ in size (micro-chip to macro-well plates), are difficult to handle and contain different surface chemistry for cell growth (e.g. PDMS), limited endpoint measurements and low throughput [7, 17, 18].

CELLBLOKS® is a patented (GB2553074B), open-top multi-chambered organ-on-a-chip platform (Fig. 1). The platform is designed in a standard SBS footprint consisting of four lines of three interconnected chambers, and in each chamber is inserted a cell growth block (see platform technical specifications Figure S1). Each cell growth block serves as an individual block in which different cells can be seeded. Three different kinds of blocks suitable for different cell types are available and include Barrier Blocks™, Circulatory Blocks™ and Blank Blocks™. Barrier blocks™ are used to emulate barrier functions such as gastrointestinal (GI) tract and blood–brain barrier (BBB), whereas Circulatory blocks™ mimic tissues in systematic

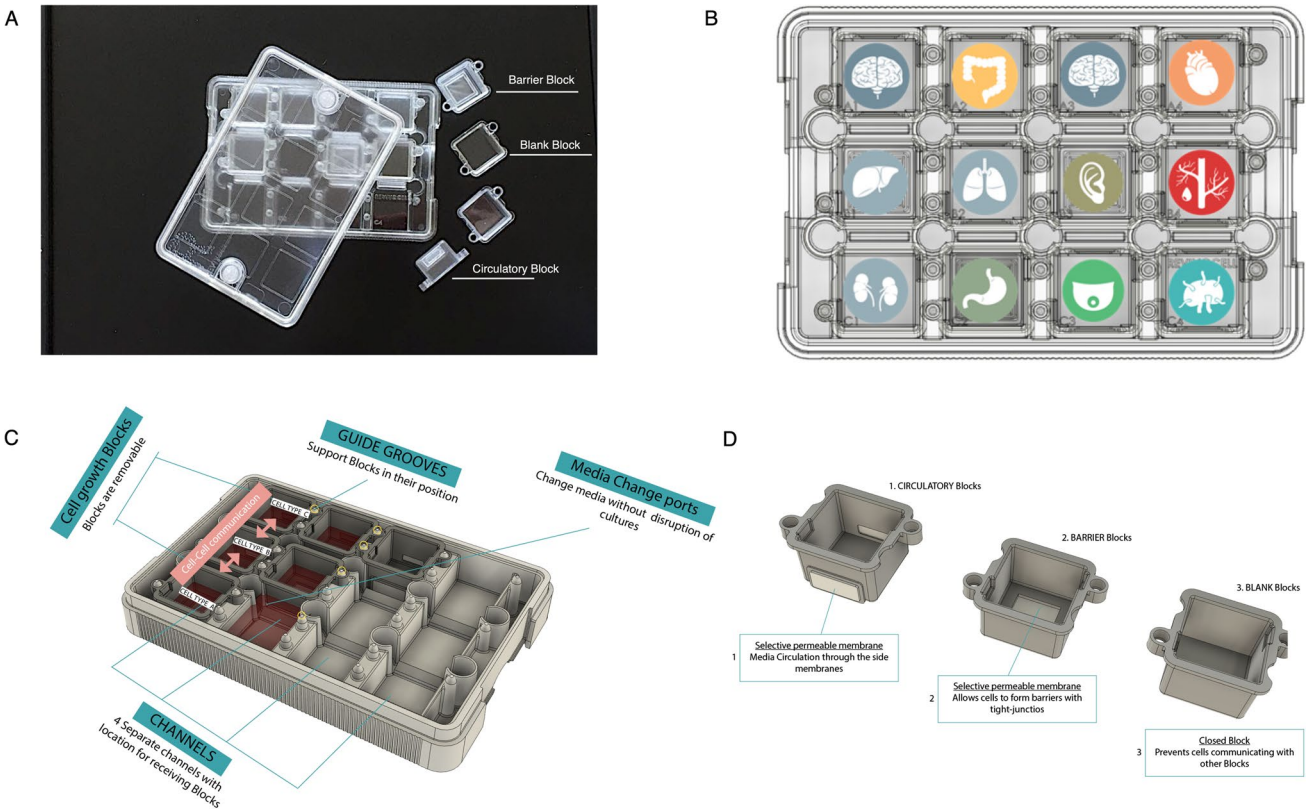

Fig. 1 Illustration of the CELLBLOKS® platform. The platform has the dimensions of a standard tissue culture well plate and is designed to allow multiple organ-specific cells/tissues to grow in separate compartment blocks (A and B). These are interconnected via cell growth blocks that maintain cells in their respective compartments but allow non-contact cell–cell communication via media flow channels (C). CELLBLOKS.® base chamber has four separate elongated channels with location for three separate cell growth blocks. Each channel is filled with media (3–5 ml) to allow the cell–cell communication between the blocks. Three types of blocks are used to mimic different tissue-specific conditions (D). 1. Circulatory blocks provide a bottom surface for cells to grow and side circulatory windows in the walls allowing selective media diffusion (both inlet and outlet, simulating organs in systematic circulation, e.g. the liver, brain, heart, lung); 2. Barrier blocks contain a selective permeable membrane on the bottom of the block, allowing cells to proliferate on a basolateral membrane (simulating epithelial cells and tissues); and 3. Blank blocks have the same surface as the circulatory blocks for cell growth but no inlet or outlet for media diffusion. Blank blocks are used to isolate cell cultures from other compartments and are often used as controls

circulation. Blank blocks™ are used to isolate cell compartments which are often used as control. The cell culture blocks are connected via channels, from which flows the culture medium between them. In the CELLBLOKS® platform, each cell block can be examined separately, and different cell types can be added or removed to the system any time during the study. This can be done in a non-destructive manner, enabling versatility to building optimal organ-specific models and monitoring model performance in real-time.

Herein, we have used CELLBLOKS® to grow various cell types that simulate liver tissue architecture in a connected interactive co-culture liver model. We hypothesise that in such settings, the crosstalk between the hepatocytes, fibroblasts and endothelial cells will enhance hepato-cellular metabolic functions compared to conventionally grown hepatocyte mono-cultures and provide more hepatic-relevant model for drug screening. The liver model was established by using HepG2 hepatocytes, an extensively studied cell line in drug safety screening [19, 20] combined with NIH/3T3 fibroblasts and human umbilical vein endothelial cells (HUVEC) that are reported to support the functions of hepatocytes in several co-culture studies [15, 21–28]. Although primary hepatocytes are preferred for biotransformation studies as more in vivo relevant, they are not readily available, exhibit high donor-to-donor variability and lose metabolic activity rapidly over long-term culture [29, 30], though attempts have been made in the last decade to stabilise their function by incorporating them into 3D cell culture and co-culture approaches [31, 32]. In contrast, HepG2 hepatocytes are an extensively used cell line in drug safety screening due to their ability to express phase II genes, affordability, easy handling and expansion for high-throughput screening; this maintains a relatively reproducible human system [19, 20]. Whist 3T3 cells are murine origin embryonic fibroblasts, they have been shown to induce higher level of function and phylotypic stability over longer period of times in human primary hepatocytes (HPH) compared to human-derived sinusoidal endothelial cells, hepatic stellate cells or Kupffer cells [33–35] possibly due to their ability to robustly express cross-species diverse molecules such as decorin and T-cadherin expressed in the liver [36]. One of the critical functions of hepatocytes in the liver is the synthesis of albumin, a protein of 585 amino acids known to play a critical role in the binding and transport of drugs, maintenance of colloid osmotic pressure and the scavenging of free radicals [37, 38]. In this study, we used albumin production, CYP estimation and urea production to optimise CELLBLOKS® liver model functions. We have also studied the toxicology profile of one of the known DILI compounds, tamoxifen, to estimate the IC_{50} values in the CELLBLOKS® liver model.

Material and methods

Cell culture

Human hepatic carcinoma (HepG2) cells, human umbilical vein endothelial (HUVEC) cells and mouse fibroblast (NIH/3T3) cells were purchased from Sigma-Aldrich™. HepG2 cells and NIH/3T3 cells were cultured in T25 cell culture flasks at 37 °C and 5% CO_2 in Dulbecco's Modified Eagle Medium (DMEM) (Gibco) supplemented with 10% (v/v) of foetal calf serum (FCS) (Thermo Fisher), 2 µM L-glutamine (Sigma-Aldrich), 100 IU/mL penicillin (Sigma-Aldrich) and 100 µg/mL streptomycin (Sigma-Aldrich). HUVECs were cultured in T25 cell culture flasks at 37 °C and 5% CO_2 in an Endothelial cell Growth Media (EGM) (Cell Application). The media was changed every 2 days and cell passaged twice weekly.

Liver modelling customisation in CELLBLOKS® platform

The human liver model is depicted using the CELLBLOKS® platform (Figs. 1 and 2). Hepatocytes (HepG2 cells), endothelial cells (HUVECs) and fibroblasts (NIH/3T3 cells) are seeded in tri-culture, co-culture and mono-culture combinations to investigate various cell combinations to optimise liver function (Fig. 2A). Circulatory blocks™ that allow exchange of media components between cell block compartments were selected and were inserted in chambers: [A1 − B1 − C1], [A2 − B2], [A3 + B3], [A4 + B4] to allow the testing of 2-way or 3-way co-culture set-up combinations. Blank blocks™ were inserted in chambers [C2], [C3] and [C4] to isolate cells (no media exchange) from other cell block compartments; these latter were used as mono-culture controls for each individual cell type. Cells in Circulatory blocks™ can communicate through 1-µm polycarbonate selectively permeable membrane windows incorporated into each block, via media circulation in the interconnected chambers (Fig. 2A, red arrows). In contrast, cells in Blank blocks™ are isolated from other cultures and cannot communicate with other cell types. These blocks are designed to study mono-culture controls with no co-culture or flow interactions in the same experimental system.

To prepare the co-culture blocks, 1 ml of cell suspension of 5×10^4 cells/well for each cell line (HepG2, NIH/3T3 and HUVEC) were seeded into each interconnected cell blocks with HepG2 on the first row, NIH/3T3 on the second row and HUVEC on the third row with 3 ml of mixed growth medium (DMEM and EGM) added to the circulating channels around the blocks. For the

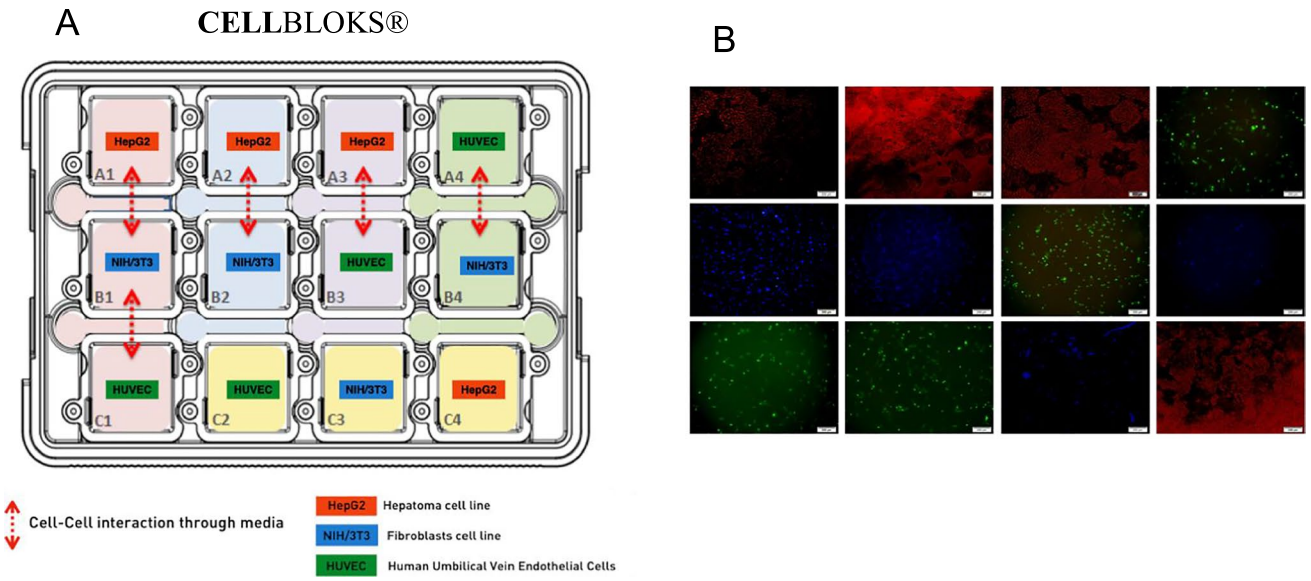

Fig. 2 Liver model set-up on CELLBLOKS® platform (**A**) and images of different cells in their respective cell growth blocks (**B**). In CELLBLOKS.® platform co-cultures were set-up using Circulatory blocks with 1.0-µm pore size PC membrane. Cell–cell interactions were tested in a tri-culture [A1–B1–C1], set of two combinations [A2–B2], [A3–B3] and [A4–C4] and in isolation to determine which cell–cell combinations produced optimal hepatic relevance. Each cell type was also grown in isolation at the same time in Blank blocks in [C2], [C3] and (C4) compartments. Cells were imaged in day 5 after culture in their respective platform using an Olympus IX73 Inverted Microscope, magnification × 10: HepG2 cells (red), HUVECs (green) and NIH/3T3 cells (blue)

mono-culture, 1 ml of cell suspension of 5×10^4 cells/well of each cell line was seeded separately on the isolated blocks of CELLBLOKS® plate. Cell viability, albumin and cytochrome P450 3A4 (CYP3A4) were measured every 2 day for 14 days.

Viability assay

Viability of the three cell lines (HepG2 cells, HUVECs and NIH/3T3) was measured simultaneously in the CELLBLOKS® platform for up to 14 days (Fig. 3).

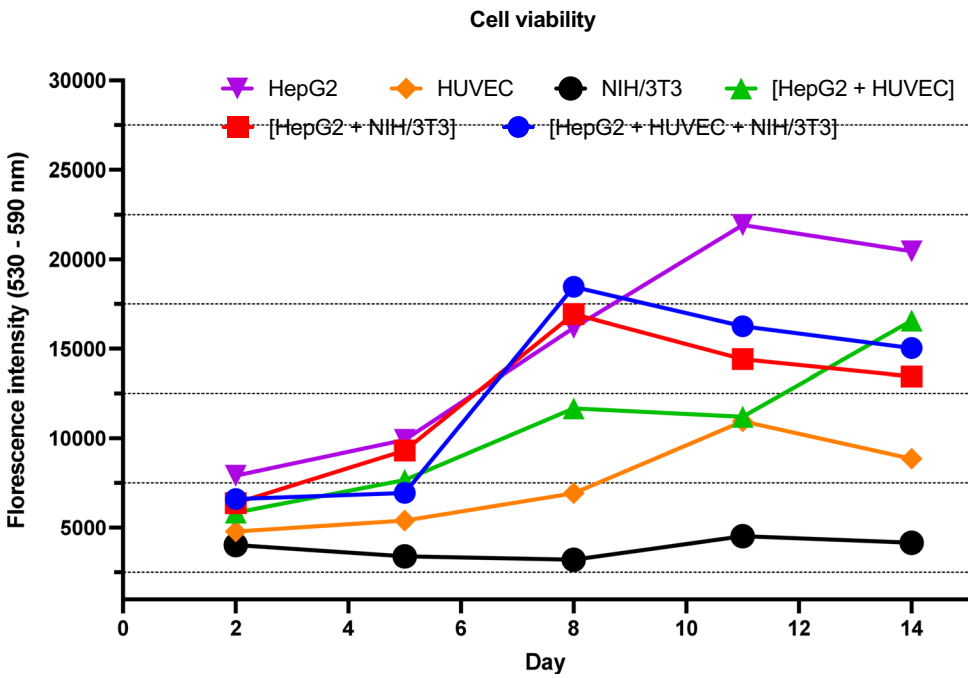

Fig. 3 Viability of different cell types and co-culture set-ups on CELLBLOKS® platform. Viability was measured in all cell types in mono-cultures, HepG2 cells, NIH-3T3 cells and HUVECs, as well as in HepG2 cells co-cultured with NIH-3T3 cells [HepG2 + NIH/3T3], HepG2 cells co-cultured with HUVEC [HepG2 + HUVEC] and in tri-culture [HepG2 + HUVEC + NIH/3T3] ($n = 3$)

Cell viability was assessed using the Alamar Blue cell viability assay (Thermo Fisher). A stock solution was prepared according to manufacturer's instructions and diluted to a working (AB) solution in a Hank's balanced salt solution (Sigma-Aldrich K) and kept at 37 °C. After the incubation time, the culture media were removed, and the cells were washed twice with PBS. To detriment viability of individual cell types in co-culture set-ups, 1 ml of the diluted AB solution (10% in Hank's solutions) was added into each block, and the plates were incubated at 37 °C and 5% CO_2 for 1 h. After incubation, aliquots of 100 µl from these blocks and wells were transferred into a 24-well plate for reading. The intensity was read by a Synergy H1 microplate reader from BioTek (Excitation 530 nm; Emission 590 nm) and analysed with Gen5 software. The cells were then washed with 1 ml of PBS three times, and 1 ml of media was added. The plates were re-incubated at 37 °C and 5% CO_2.

Imaging

HepG2 cells and HUVEC were stained with the Cell Tracker Red CMTPX (Thermo Fisher Scientific) and the Cell Tracker Green CMFDA (Thermo Fisher), respectively, on day 0 of the experiment (Fig. 2B). The cells were cultured in T25 flasks in appropriate media. To prepare the working solution, cell trackers were diluted in dimethyl sulfoxide (DMSO) (Sigma-Aldrich) to a final concentration of 10 mM and finally in serum-free media (SFM) (Gibc) to a final concentration of 10 µM. Once the cells were confluent, the media was removed from the flasks, cells were washed twice with PBS, and the working solution of cell tracker was gently added (Red Cell Tracker to HepG2 cells and Green Cell Tracker to HUVEC). The cells were incubated at 37 °C and 5% CO_2 for 45 min. After the incubation, the solution from the cells was removed, and the cells were washed twice with PBS and trypsinised with 2 mL of trypsin (0.05%) for 7 min prior to being seeded in 12-well plate or CELLBLOKS® platform according to the experimental plan. On day 1, 2 µM of Hoechst solution (Sigma-Aldrich) was added to each well. The cells were imaged with an Olympus IX73 Inverted Microscope (Olympus) using magnification × 10, with Olympus CellSens standard software. Images were processed with ImageJ software.

Albumin assay

Albumin production from each cell growth block containing HepG2 cells was determined using the Bromocresol Green (BCG) Albumin assay kit (MAK124, Sigma-Aldrich). Albumin standard curves were first calculated according to the vendor's protocol. Cells were scraped from each block into 1-ml separate centrifuge tubes and counted using a haemocytometer. For each condition, cells were lysed in 100 µl of cold lyses buffer for 60 min at 4 °C. The cell solution is centrifuged at 13,000 g for 10 min at 4 °C to remove insoluble material. In each well of a 96-well plate, 10 µl of sample supernatant (or a standard) and 200 µl of albumin reagent are added according to the supplier's indication. The absorbance at 450 nm was measured with a Synergy H1 microplate reader from BioTek and analysed with Gen5 software. The assay is conducted in triplicate at different time points: day 1, day 4, day 8 and day 12 of culture.

Urea assay

The biosynthetic capabilities of HepG2 cells were assessed using a Urea Assay Kit (MAK006, Sigma-Aldrich™). A standard curve was interpolated, and urea production was measured according to the supplier's instructions. Cells were first scraped form each block into 1 ml separate centrifuge tubes and counted using a haemocytometer. Then for each condition, HepG2 cells were lysed in 100 µl of cold lyses buffer for 60 min at 4 °C. The cell solution was centrifuged at 13,000 g for 10 min at 4 °C to remove insoluble material. In each well of a 96-well plate, 50 µl of sample supernatant (or standard) and 50 µl of enzyme reaction mixes (peroxidase substrate, enzyme mix, developer and converting enzyme) are added according to the supplier's indication.

The absorbance at 570 nm was measured with a Synergy H1 microplate reader from BioTek and analysed with Gen5 software. The assay was conducted in triplicate at different time points: day 1, day 4, day 8 and day 12 of culture.

Cytochrome P450 assay

CYP3A4 expression in HepG2 cells was measured with a P450-Glo assay (V9001 Luceferin-IPA, Promega). Cells were scraped from each block into 1 ml PBS tubes and counted using a haemocytometer. Cells were then placed in 96-well opaque plates and the assay was performed according to the supplier's instructions. Luminescence was measured with a Synergy H1 microplate reader (BioTek™) and analysed with Gen5 software. The assay was conducted in triplicate at different time points: day 1, day 4, day 8 and day 12 of culture.

Tamoxifen toxicity on tri-culture versus mono-culture hepatocytes

All dilutions were prepared using sterile culture media in a sterile culture hood. To prepare the tri-culture blocks, 1 ml cell suspension of 5×10^4 cells/well for each cell line (HepG2, NIH/3T3 and HUVEC) was seeded into the interconnected Circulator blocks™ with HepG2 on the first row, NIH/3T3 on the second row and HUVEC cells on the third row with 3 ml mixed growth medium (DMEM and EGM)

added to the circulating tunnels around the blocks; these were incubated for 24 h. For the mono-culture, 1 ml cell suspension of 5×10^4 cells/well of only the HepG2 cell line was seeded on the isolated Blank blocks™ of a CELLBLOKS® platform. Treatment with different tamoxifen concentrations (0.1 µM, 1 µM, 10 µM, 50 µM, 100 µM) for each cell line using DMSO as control, 60 µL of DMSO was added to the first row (HepG2, NIH/3T3 and HUVEC) by adding 10 µl to each block and 30 µl in the circulating medium. For the drug treatment, the same sequence was followed (60 µl of each drug concentration was distributed between blocks and circulating medium) and then incubated for 24 h. Cytotoxicity of tamoxifen was measured on HepG2 cells using CellTiter-Glo® Luminescent ATP Cell Viability Assay (G7570, Promega), and the assay was performed according to the manufacturer's protocol. Briefly, the plates with its contents were equilibrated to room temperature for approximately 30 min, and then the media was removed from each block and replaced with 200 µl fresh media and 200 µl of CellTiter-Glo® reagent (CellTiter-Glo® Buffer plus CellTiter-Glo® lyophilised substrate) and incubated at room temperature for 10 min. Luminescence was recorded using a microtiter plate reader. Cell viability was expressed in percentages in comparison to control (DMSO treated) ($n = 12$).

Statistical analysis

All statistical analysis were performed using GraphPad Prism (V9.3.1). Analysis of statistical significance comparing urea, albumin and CY3A4 in mono-cultures versus co-culture and tri-culture conditions were calculated using two-way multiple comparisons ANOVA. A P value of $^*P \leq 0.05$ was set as a threshold for statistically significant results. IC_{50} values of tamoxifen dose–response curves were measured using non-linear four-parameter variable slope model, log (inhibitor) versus response.

Results

Cell viability was determined in cell growth blocks for a period of 14-day culture and shows that the platform supports cell growth with different mono-cultures and co-cultures that vary in their growth rate and patterns (Fig. 3). In general, HepG2 mono-cultures grow at higher rate compared to both HUVEC and NIH/3T3 mono-cultures, and this is apparent in the 2-week duration of cell growth tests. HepG2 cell viability alone shows a gradual temporal viability increase from day 2 to day 11, after which they start to decline (Fig. 3). When HepG2 cells are connected in co-culture with HUVECs, viability increases continuously from day 2 to day 8 and decreases slowly after day 8. The viability curve of HepG2 cells connected with NIH/3T3 cells has the same pattern; cells grow rapidly between day 5 and day 8 of culture, and viability decreases slowly after day 8. Finally, HepG2 cell growth in tri-culture with HUVECs and NIH/3T3 cells is initially slow during the first 5 days of co-culture, and then cell viability increases rapidly until day 8 and decreases slowly in a similar pattern to other co-culture combinations (Fig. 3).

Imaging of cells through the platform was achieved by pre-labelling each cell type with different cell trackers (HepG2 cells in red, HUVEC cells in green and NIH/3T3 cells with the DNA intercalating agent Hoechst in blue) before seeding into the cell growth blocks. Figure 2B shows live imaging of cell compartments within each cell growth block where cells were labelled directly without being disturbed. Tracking of cells with time indicated that cells seeded independently remain in their blocks and are unable to pass through membrane to other cells' compartments. This allowed each cell type to be studied individually without cross-contamination.

Following assessment of viability and imaging of cells in the platform, the levels of urea, albumin and CYP3A4 activity were measured in HepG2 hepatocytes only at different time points to determine hepatic relevance effected by different cell combinations, and two-way multiple comparison ANOVA was used to statistically compare mono-culture values vs. all other co-culture and tri-culture conditions (Figs. 4–6). Overall, urea production per cell was generally higher in days 1 to 4 of culture in all conditions but decreased in a time-related fashion after day 4 with the lowest levels of expression noted on day 12 (Fig. 4). At day 1, urea levels remain similar in mono-cultures as well as other co-culture and tri-culture conditions. However, at day 4, the urea produced in co-cultures is significantly higher compared to HepG2 mono-cultures; urea expression is doubled by the presence of HUVEC cells (~40 pg/cell) and tripled by the presence of NIH/3T3 fibroblasts (~60 pg/cell) co-cultures, respectively. However, in tri-cultures (HepG2 + HUVEC + NIH/3TR), the urea level of ~30 pg/cell is noted, although this is not statistically significant ($P = 0.3$). Following 4-day culture, no statistical difference between mono-cultures and other co- and tri-culture conditions is noted, and urea levels seem to drastically decrease with time; urea produced per cell at day 8 decreased by at least half in all conditions, with day 12 showing the lowest levels of less than 10 pg/cell.

Similarly, albumin levels are at their highest in the first 4 days of culture, and then their levels fall away after day 5; this is apparent in all culture conditions (Fig. 5). Co-cultures induce a significant increase in albumin levels compared to HepG2 cells cultured independently on day 4 of culture. However co-cultures do not appear to improve albumin production in the first 24 h of incubation, where a reduction of albumin levels is observed in the presence of NIH/3T3 fibroblasts where albumin inhibition is noted in HepG2 + NIH/3T3 co-cultures and tri-cultures of HepG2 + HUVEC + NIH/3T3.

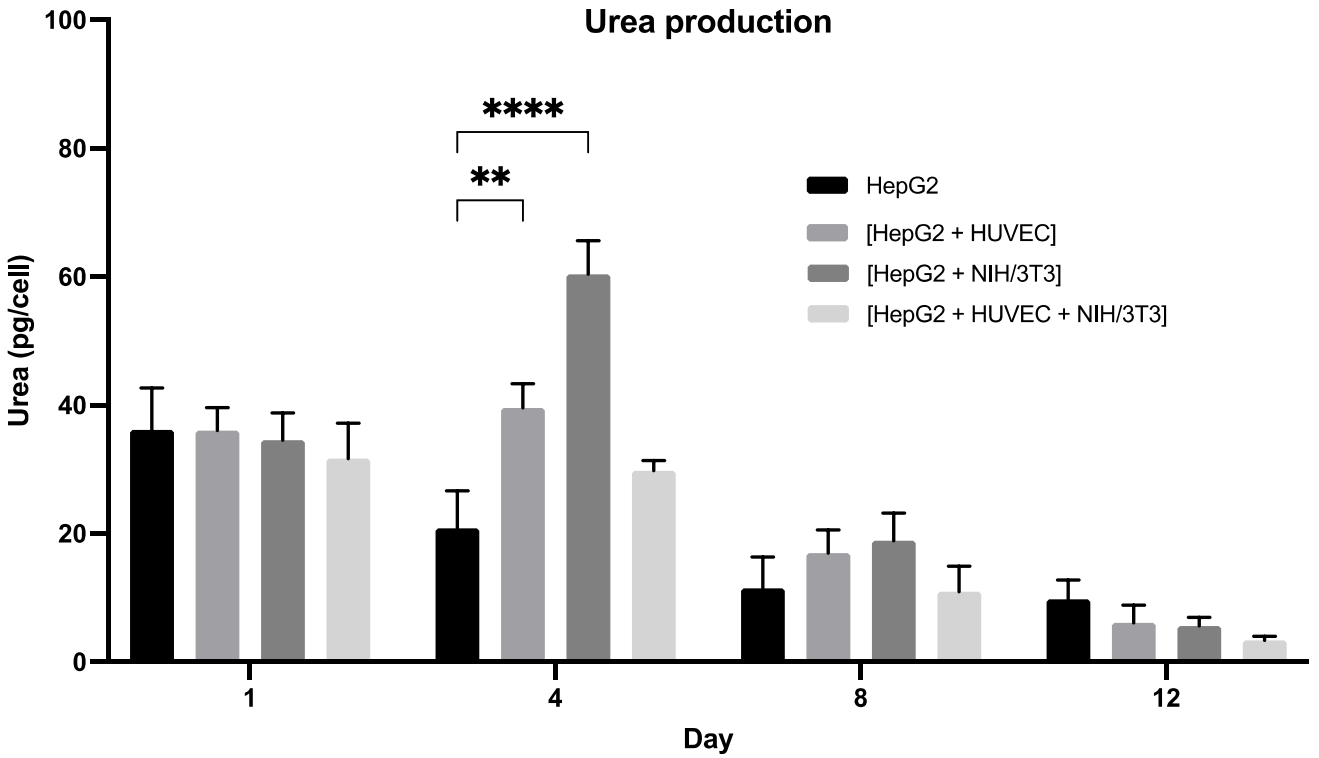

Fig. 4 Urea production in HepG2 cells in mono-cultures and in different co-culture and tri-culture conditions. Urea was measured in HepG2 cells alone (HepG2), HepG2 cells co-cultured with NIH-3T3 cells [HepG2 + NIH/3T3], HepG2 cells co-cultured with HUVECs [HepG2 + HUVEC] and in tri-culture [HepG2 + HUVEC + NIH/3T3] ($n = 3, \pm$ SEM). Urea production in HepG2 mono-cultures was compared to co-cultures and tri-cultures, respectively, using two-way ANOVA in GraphPad Prism 9 (*$p \leq 0.05$, **$p \leq 0.01$, ***$p \leq 0.001$)

In contract, there are no inhibitory effects of HUVEC cells on HepG2 albumin levels. However, following day 4 of culture, albumin production drastically drops in HepG2 mono-cultures from 25.6 pg/cell down to 6.2 pg/cell but remain significantly higher in co-cultures indicating enhancement of albumin levels over longer-term culture. In contrast to HepG2 mono-cultures, albumin levels are nearly tripled in the presence of NIH/3T3 cells (23.0 pg/cell vs. 6.2 pg/cell) and doubled in co-culture with HUVEC cells (14.0 pg/cell). However, in tri-cultures, the cell–cell interactions appear to reduce albumin expression to 9.3 pg/cell compared to HepG2 in co-culture with HUVEC or NIH/3T3 separately, indicating a combined interplay of endothelial cells with fibroblasts in down-regulating albumin levels.

In all cell growth conditions, CYP activity per cell remains high in the first 24 h of culture, but expression levels reduce significantly after this point (Fig. 6). All co-culture conditions significantly improve CYP3A4 expression following 24 h of co-culture; HUVEC and NIH/3T3 cells stimulate HepG2s to double CYP3A4 production from 21.6 ng/cell to 44.3 pg/cell and 45.9 pg/cell, respectively. However, in tri-culture (HepG2 + HUVEC + NIH/3T3), the levels of CYP3A4 expression enhanced the highest compared other co-culture where the levels are tripled compared to HepG2 mono-cultures to 67.1 pg/cell. At day 4 of culture, CYP3A4 activity per/cell reduces drastically compared to the first 24-h levels indicating enhanced metabolic activity in the initial cell synthesis phase.

Tamoxifen-induced dose–response effects in both HepG2 cells cultured alone and in HepG2 cells cultured in combination with HUVEC and NIH/3T3 cells, with the lowest observed effects at 0.1 µM and more than 90% cell death at > 50 µM concentrations (Fig. 7). However, the dose–response curve varied with each cell model. HepG2 cells in tri-culture exhibit higher sensitivity to tamoxifen treatment at lower concentrations < 5 µM compared to HepG2 mono-cultures. Additionally, the IC_{50} value for HepG2 mono-cultures is double (16.40 versus 8.96) that of HepG2 cells in tri-culture, indicating a higher sensitivity to tamoxifen toxicity.

Discussion

The main objective of this study is to demonstrate the capability of a new organ-on-a-chip platform (CELLBLOKS®) that can be used to create organotypic cell culture conditions in standard laboratory settings and test complex cell–cell interactions that give optimal

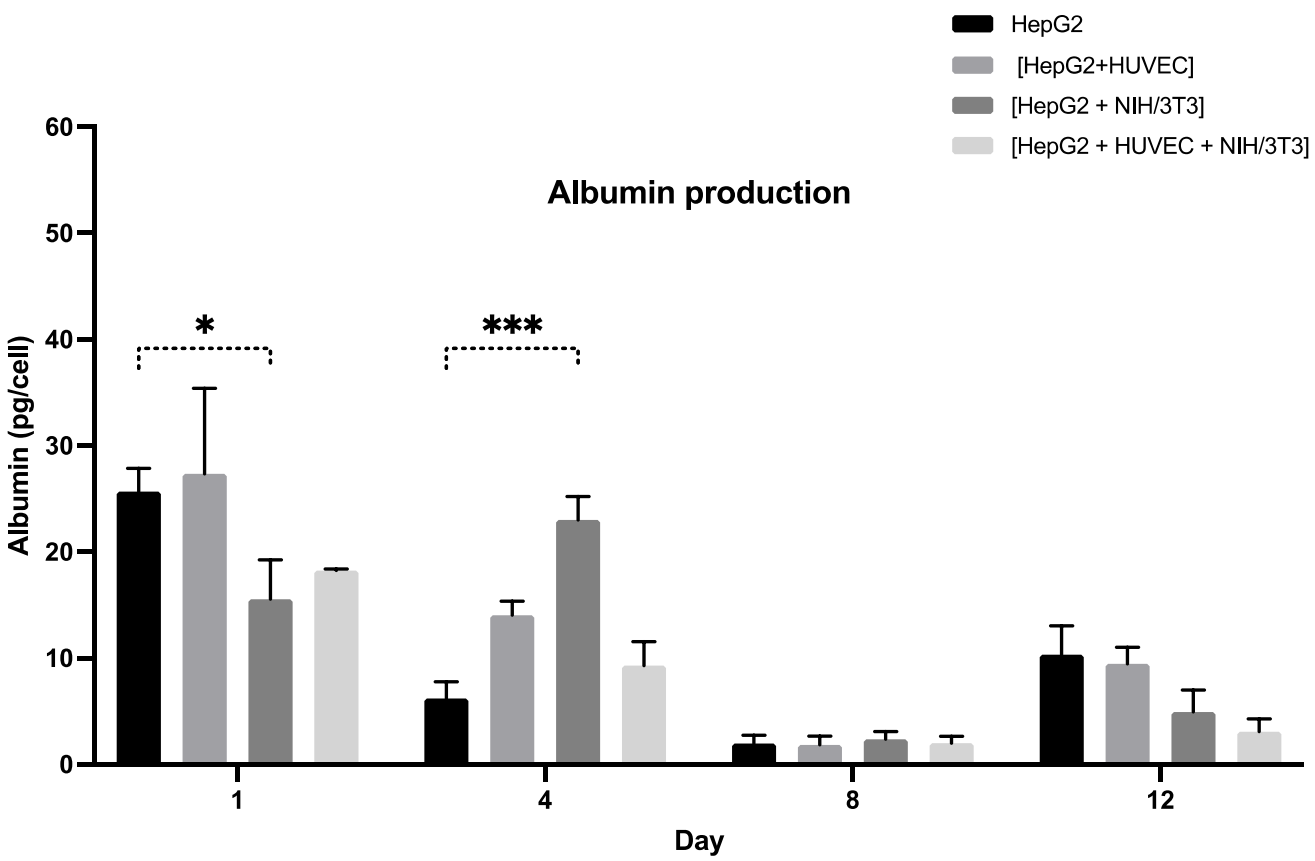

Fig. 5 Albumin production in HepG2 cells in mono-cultures and in different co-culture and tri-culture conditions. Urea was measured in HepG2 cells alone (HepG2), HepG2 cells co-cultured with NIH-3T3 cells [HepG2 + NIH/3T3], HepG2 cells co-cultured with HUVEC [HepG2 + HUVEC] and in tri-culture [HepG2 + HUVEC + NIH/3T3] ($n = 3, \pm$ SEM). Albumin levels in HepG2 mono-cultures were compared to co-cultures and tri-cultures, respectively, using two-way ANOVA in GraphPad Prism 9 (*$p \leq 0.05$, **$p \leq 0.01$, ***$p \leq 0.001$)

biological relevance. We used the platform's "plug-and-play" approach to model the liver in vitro so that it can predict drug-induced hepatotoxic effects in humans more accurately during preclinical testing stages. The liver is a complex organ that involves the interplay of multiple cell types including hepatocytes, endothelial, fibroblast, bile duct epithelial and Kupffer cells [39]. CELLBLOKS® allows one to explore how heterogeneous interactions of different liver cell types drive hepatic relevance. The platform enables precise control of ratios between different cell types allowing various cell–cell interaction studies as well as facilitating the relative proximity between different cell types relevant to in vivo locations. In addition, each cell population is grown in different compartments allowing cell proliferation in a specific required culture condition, which may be different from another cell type. Once the required cellular growth of each cell type is achieved, the cell growth blocks can be plugged in the platform for inoculating the co-culture. This particularly feature is useful with cells sensitive to media changes and having different growth rates.

Other recent methods for modelling liver in vitro include microfluid-chip approaches that also take into account controlled media perfusion in the cultures. Hepatocytes in the liver are not subjected to direct blood flow and are protected from flow-induced shear stress by endothelial cells that fenestrate in the capillary sinusoid wall allowing exchange of O_2, CO_2 and metabolites [40]. Although the introduction of flow can improve nutrient supply and induce O_2 zonation, hepatocytes might also be subject to damage if the flow rates are too high [41, 42].

In CELLBLOKS® liver model, the HepG2 cells are divided by a thin permeable membrane that allows metabolite and gas exchange between cells and the culture medium via passive diffusion, and the flow is provided using the CELLBLOKS® channels. All the three cell types (HepG2, fibroblasts and endothelial cells) retain high levels of cell viability, possess excellent cellular morphology and exhibit significantly enhanced liver functions compared to their counterparts in standard mono-cultures. The data suggests that the differentiation of HepG2 cells has enhanced due to cellular interaction with other cell types (endothelial

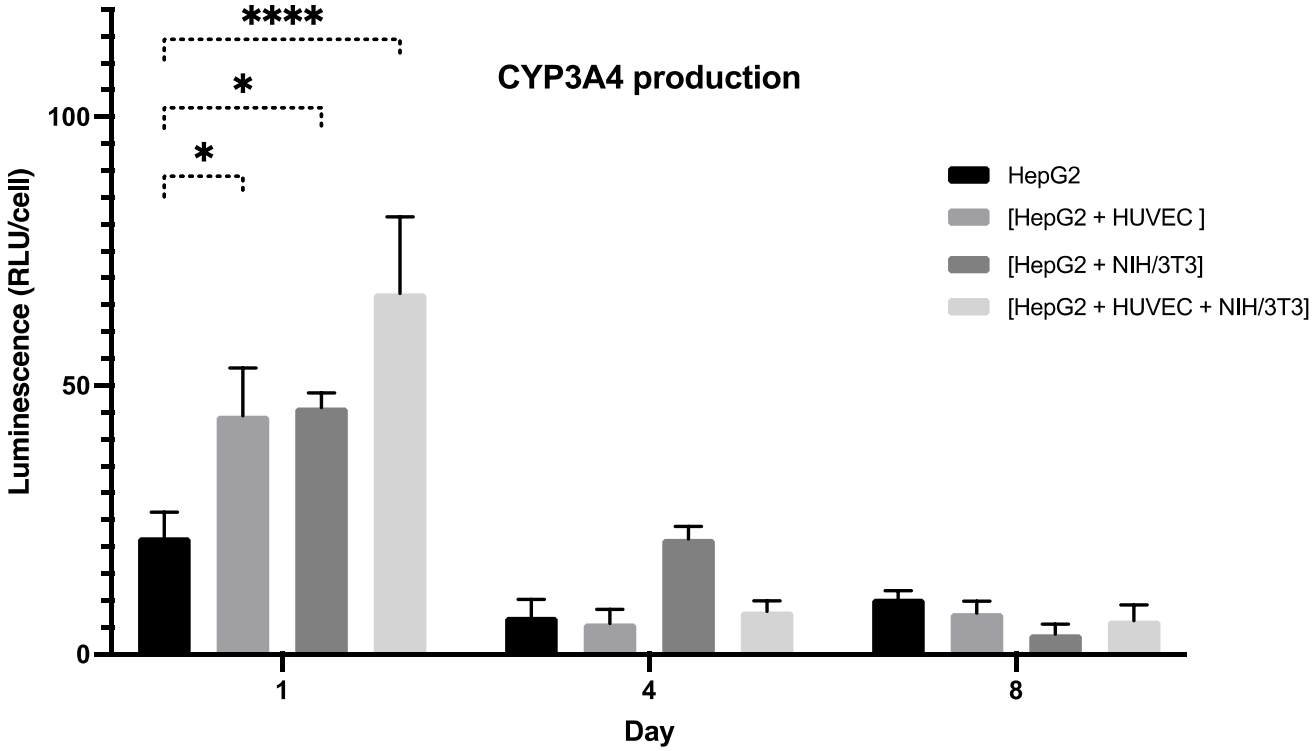

Fig. 6 CYP3A4 production in HepG2 cells in mono-culture and in different co-culture and tri-culture conditions. CYP3A4 was measured in HepG2 cells alone (HepG2), HepG2 cells co-cultured with NIH-3T3 cells [HepG2 + NIH/3T3], HepG2 cells co-cultured with HUVEC [HepG2 + HUVEC] and in tri-culture [HepG2 + HUVEC + NIH/3T3] ($n = 3, \pm$ SEM). CYP3A4 levels in HepG2 mono-cultures were compared to co-cultures and tri-cultures, respectively, using two-way ANOVA in GraphPad Prism 9 ($^{*}p \leq 0.05$, $^{**}p \leq 0.01$, $^{***}p \leq 0.001$)

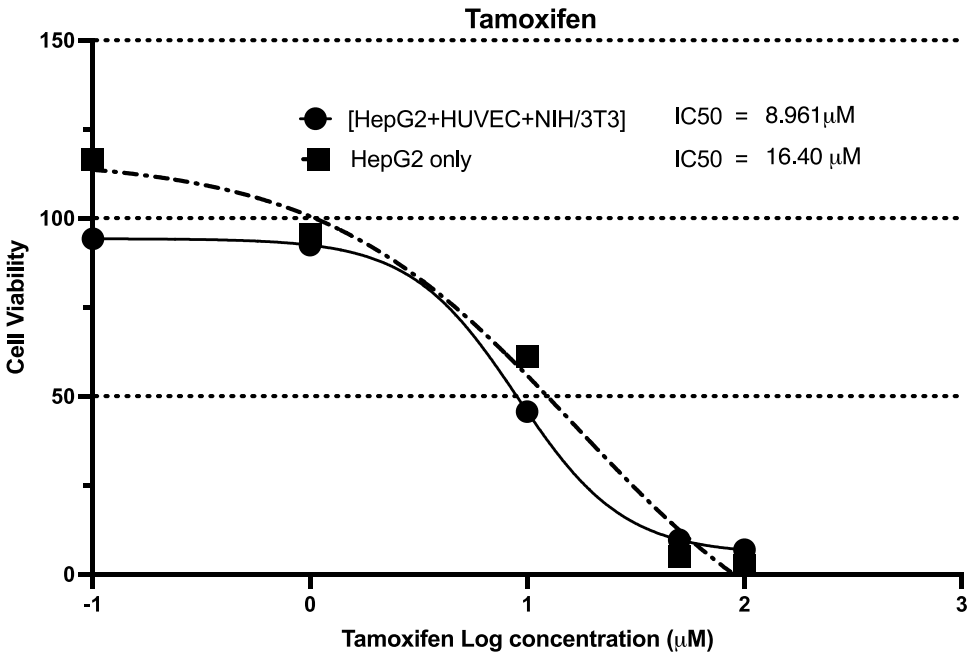

Fig. 7 IC_{50} in mono-cultures (HepG2, $R^2 = 0.887$) versus tri-culture (HepG2 + HUVEC + NIH/3T3, $R^2 = 0.9354$) in CELLBLOKS.® platform calculated using GraphPad Prism 9, non-linear four-parameter variable slope models. Cytotoxicity is HepG2 cultured alone in mono-cultures compared to HepG2 cells grown in connected tri-cultured, following 24-h exposure to tamoxifen. All experiments were conducted in triplicate ($n = 3$)

and fibroblast) and the flow system provided by the CELLBLOKS® platform. Further to that, the liver function in co-culture of all three cell types is significantly improved compared to mono-culture hepatocytes; this includes albumin protein production, CYP450 expression and urea synthesis; this highlights the need for their inclusion in liver

modelling to mimic physiological relevant human liver. Though the CYP activity of HepG2 cells was high in the first 4 days of culture, a subsequent decline was observed, which is in line with Duthie and Collins' study that reported reduced glutathione content dramatically increases at 24 h of HepG2 cell culture and declined after 1 day of culture when cells approach confluence [43]. Although HepG2 cells express low amounts of CYP compared to HepRG and primary hepatocytes, they are still used in different drug screening programs due to being well-established, widely available and extensively studied compared to other cells [21, 25, 44, 45]. Compared to conventional mono-cultured HepG2 cells, both co-cultures and tri-cultures set-ups stimulated an increase of CYP3A4 metabolic activity by up to three times indicating an improved in vitro liver model. Given that CYP450 enzymes are important in drug metabolism and drug–drug interactions and are commonly used to measure drug-induced cellular responses [46], the tri-culture model (HepG2 + HUVEC + NIH/3T3) was selected to examine tamoxifen toxicity as this model exhibited the highest CYP3A4 compared to other co-culture and mono-culture set-ups.

This study highlights that in contrast to mono-cultures, the hepatic phenotype can be enhanced and stabilised significantly by non-contact co-culture with non-liver-derived nonparenchymal cells (NPCs) even in monolayers without necessitating the need of spheroid/aggregate formation. In addition, the simple 2D set-up enables high content imaging such as epifluorescence microscopy and high-throughput screening, and therefore, this platform provides added value that is compatible with existing workflow environments in drug discovery programs. The incorporation of normal human primary hepatocytes in similar co-culture set-up with liver NPCs including hepatic stellate cells, liver sinusoidal endothelial cell and Kupffer cells combined with 3D extracellular matrix environments is likely to provide more in vivo relevant outputs and added value in DILI predictions.

CELLBLOKS® platform allows one to perform experiments on any seeded cell type separately. This allows for each cell type to be unpluged from the system any time during or after the experiment to study the effect separately. For example, we have studied hepatocyte metabolism in the HepG2 cell only from the pool of fibroblast and endothelial cells. Additionally, each cell type can be further analysed separately following a combined exposure to similar treatment regimes. This is particularly useful in understanding chemical mode of action at organ level rather than just the individual cell type. This feature is possible in the CELLBLOKS® platform but not feasibly in randomly mixed co-culture models. For example, using our technology we analysed for liver function (i.e. albumin production, urea excretion and CYP activity) separately after co-culturing the three cells for 14 days. This is important when albumin is also expressed in extra-hepatic tissues [47] and urea is produced by HUVECs via arginase activity [48], and that may reduce the bias induced by the mix of two or three cell lines in the wells. In addition, tamoxifen toxicity when compared in mono-culture and tri-culture (HepG2 separated analysis after culture) appeared to be increased in tri-cultured hepatocytes compared to mono-cultured hepatocytes indicating of increased sensitivity to toxic insult with this model.

The CELLBLOKS® platform is a new promising cell culture device used for modelling cell-to-cell and organ-to-organ interactions. In this study, we have concentrated on cell-to-cell interactions to develop a liver model, but the design of interconnected chambers allows organ-to-organ communication. The 3D organ/organoids (e.g. gastrointestinal tract, liver) are grown separately and then plugged together in combined culture conditions. For instance, Barrier blocks™ containing selective membrane at the bottom can be used to create barrier functions (i.e. gastrointestinal tract or blood–brain barrier), whereas Circulatory blocks™ are applied to simulate for non-barrier organ functions. The Blank blocks™ are used in isolating cultures as controls to study their function compared to connected interacting cells.

Furthermore, seeding the cells in independent compartments makes experiments easier while maintaining communication via soluble factor excretion. When tri-cultures or co-cultures are carried out, assays can be performed only with the cell line of interest. Another advantage is the compatibility of the plate with readout equipment such as microscopes and plate readers as well automated handling applied in high-throughput screening (HTS). Moreover, the "plug-and-play" deign makes it easy to use, like a conventional well plate; its utilisation is easier than complex microfluidic systems.

The CELLBLOKS® is designed to explore crosstalk between tissues and cells in separate cultures. In this system, different types of cells can be cultured individually but connected through the flow of the medium via passive diffusion. Alternatively, gravity-driven flow can be induced within and between the cell culture compartments using a platform rocker without the need of external pump. Such a set-up allows physiologically relevant shear stress induction of less than 2 dyn cm^{-2} on cells [49] resembling in vivo liver sinusoids levels [50, 51] while additionally enabling economic operations and preventing bubble formation which is a significant problem in microfluidic devices [52, 53].

This enables each culture to be addressed and interrogated individually. While conventional co-cultures are useful for the study and optimisation of cell function, they are not a suitable model for investigating interactions between cell types arising from different tissues. In this sense, the CELLBLOKS® platform represents a more physiological relevant model. Herein, hepatocytes' functionality when combined with endothelial cells and fibroblast in both

mono-cultures, co-cultures and tri-cultures was explored, which highlighted that cell–cell interactions produce most biological relevance. Connected cultures enhance albumin synthesis, urea production and CYP metabolic activity in hepatocytes compared to non-connected mono-cultures. Therefore, as demonstrated here, the connected culture in the CELLBLOKS® system combines the dynamic stimulus of flow with cell crosstalk through soluble ligands so that the unit production of albumin, CYP3A4 and urea is greater than in mono-cultures.

In summary, we have developed a novel device that can be used to culture cells and produce cellular models with optimal organ-specific biological relevance and enhanced physiological simulation. We have demonstrated the application of this technology for the human liver model and have shown that cellular performance can be significantly enhanced. In vitro systems that enable cells to grow in a manner more closely resembling their native counterparts will result in the development of assays that provide more accurate data about cell function which in turn will contribute to improving the efficiency of research and development. We demonstrate that CELLBLOKS® interactive "plug-and-play" approach allows one to systematically test the interactions of multiple cell types simultaneously in one platform that helps to unravel complex cell–cell interactions that drive biological relevance. In addition, we hypothesise that multiple cell-type engineering of liver model in such non-contact set-up is more advantageous for screening DILI issues compared to randomly mixed co-cultures both practically and as a predictive assay.

Supplementary Information The online version contains supplementary material available at https://doi.org/10.1007/s44164-022-00027-8.

Acknowledgements We wish to thank Innovate UK for funding this project (Grants 103006, 104432). CELLBLOKS® is a patented technology and consists of a family of patents including the UK (Granted: GB2553074B), the USA (Pending: 16/075,136), PCT (Pending: PCT/GB2017/05) and Europe (Pending: EP:1713365.9).

Data availability The datasets generated during and/or analysed during the current study are available from the corresponding author on reasonable request.

Declarations

Conflict of interest V. L., M. R. S., A. A., V. H., I. I. P. and A. R. are employees of Revivocell and may hold equity; F. L. M. is a board member of Revivocell Limited.

References

1. Hanahan D, Weinberg RA. Hallmarks of cancer: the next generation. Cell. 2011;144(5):646–74. https://doi.org/10.1016/j.cell.2011.02.013.
2. Joyce JA, Pollard JW. Microenvironmental regulation of metastasis. Nat Rev Cancer. 2009;9(4):239–52. https://doi.org/10.1038/nrc2618.
3. Koontongkaew S. The tumor microenvironment contribution to development, growth, invasion and metastasis of head and neck squamous cell carcinomas. J C. 2013;4(1):66. https://doi.org/10.7150/jca.5112.
4. Fung M, Thornton A, Mybeck K, Wu JH-H, Hornbuckle K, Muniz E. Evaluation of the characteristics of safety withdrawal of prescription drugs from worldwide pharmaceutical markets-1960 to 1999. Drug Inf J. 2001;35(1):293–317. https://doi.org/10.1177/009286150103500134.
5. MacDonald JS, Robertson RT. Toxicity testing in the 21st century: a view from the pharmaceutical industry. Toxicol Sci. 2009;110(1):40–6. https://doi.org/10.1093/toxsci/kfp088.
6. Onakpoya IJ, Heneghan CJ, Aronson JK. Post-marketing withdrawal of 462 medicinal products because of adverse drug reactions: a systematic review of the world literature. BMC Med. 2016;14(1):1–11. https://doi.org/10.1186/s12916-016-0553-2.
7. Lin C, Khetani SR. Advances in engineered liver models for investigating drug-induced liver injury. BioMed Res Int. 2016 https://doi.org/10.1155/2016/1829148
8. Zhou Y, Shen JX, Lauschke VM. Comprehensive evaluation of organotypic and microphysiological liver models for prediction of drug-induced liver injury. Front Pharmacol. 2019;10:1093. https://doi.org/10.3389/fphar.2019.01093.
9. Ballet F. Preventing drug-induced liver injury: how useful are animal models? Dig Dis. 2015;33(4):477–85. https://doi.org/10.1159/000374093.
10. Lemon R, Dunnett SB. Surveying the literature from animal experiments. BMJ. 2005;330:977–8.
11. Roth RA, Ganey PE. Animal models of idiosyncratic drug-induced liver injury—current status. Crit Rev Toxicol. 2011;41(9):723–39. https://doi.org/10.3109/10408444.2011.575765.
12. Olson H, Betton G, Robinson D, Thomas K, Monro A, Kolaja G, Lilly P, Sanders J, Sipes G, Bracken W. Concordance of the toxicity of pharmaceuticals in humans and in animals. Regul Toxicol Pharmacol. 2000;32(1):56–67. https://doi.org/10.1006/rtph.2000.1399.
13. Petrov PD, Fernández-Murga ML, López-Riera M, Goméz-Lechón MJ, Castell JV, Jover R. Predicting drug-induced cholestasis: preclinical models. Expert Opin Drug Metab Toxicol. 2018;14(7):721–38. https://doi.org/10.1080/17425255.2018.1487399.
14 Dunn JC, Tompkins RG, Yarmush ML. Long-term in vitro function of adult hepatocytes in a collagen sandwich configuration. Biotechnol Prog. 1991;7(3):237–45. https://doi.org/10.1021/bp00009a007.
15 Bhatia S, Balis U, Yarmush M, Toner M. Microfabrication of hepatocyte/fibroblast co-cultures: role of homotypic cell interactions. Biotechnol Prog. 1998;14(3):378–87. https://doi.org/10.1021/bp980036j.
16. Li CY, Stevens KR, Schwartz RE, Alejandro BS, Huang JH, Bhatia SN. Micropatterned cell–cell interactions enable functional encapsulation of primary hepatocytes in hydrogel microtissues. Tissue Eng Part A. 2014;20(15–16):2200–12. https://doi.org/10.1089/ten.tea.2013.0667.
17. Beckwitt CH, Clark AM, Wheeler S, Taylor DL, Stolz DB, Griffith L, Wells A. Liver 'organ on a chip.' Exp Cell Res. 2018;363(1):15–25. https://doi.org/10.1016/j.yexcr.2017.12.023.
18. Cui P, Wang S. Application of microfluidic chip technology in pharmaceutical analysis: a review. J Pharm Anal. 2019;9(4):238–47. https://doi.org/10.1016/j.jpha.2018.12.001.
19. Chu Q, Zhao Y, Shi X, Han W, Zhang Y, Zheng X, Zhu J. In vivo-like 3-D model for sodium nitrite- and acrylamide-induced hepatotoxicity tests utilizing HepG2 cells entrapped in

micro-hollow fibers. Sci Rep. 2017;7(1):14837. https://doi.org/10.1038/s41598-017-13147-z.
20. Wilkening S, Stahl F, Bader A. Comparison of primary human hepatocytes and hepatoma cell line Hepg2 with regard to their biotransformation properties. Drug Metab Dispos. 2003;31(8):1035–42. https://doi.org/10.1124/dmd.31.8.1035.
21. Bale SS, Vernetti L, Senutovitch N, Jindal R, Hegde M, Gough A, McCarty WJ, Bakan A, Bhushan A, Shun TY. In vitro platforms for evaluating liver toxicity. Exp Biol Med. 2014;239(9):1180–91. https://doi.org/10.1177/1535370214531872.
22. Cho CH, Park J, Tilles AW, Berthiaume F, Toner M, Yarmush ML. Layered patterning of hepatocytes in co-culture systems using microfabricated stencils. Biotechniques. 2010;48(1):47–52. https://doi.org/10.2144/000113317.
23. Evenou F, Hamon M, Fujii T, Takeuchi S, Sakai Y. Gas-permeable membranes and co-culture with fibroblasts enable high-density hepatocyte culture as multilayered liver tissues. Biotechnol Prog. 2011;27(4):1146–53. https://doi.org/10.1002/btpr.626.
24. Freyer N, Greuel S, Knöspel F, Strahl N, Amini L, Jacobs F, Monshouwer M, Zeilinger K. Effects of co-culture media on hepatic differentiation of hiPSC with or without HUVEC co-culture. Int J Mol Sci. 2017;18(8):1724. https://doi.org/10.3390/ijms18081724.
25. Gebhardt R, Hengstler JG, Müller D, Glöckner R, Buenning P, Laube B, Schmelzer E, Ullrich M, Utesch D, Hewitt N. New hepatocyte in vitro systems for drug metabolism: metabolic capacity and recommendations for application in basic research and drug development, standard operation procedures. Drug Metab Rev. 2003;35(2–3):145–213. https://doi.org/10.1081/DMR-120023684.
26. German CL, Madihally SV. Type of endothelial cells affects HepaRG cell acetaminophen metabolism in both 2D and 3D porous scaffold cultures. J Appl Toxicol. 2019;39(3):461–72. https://doi.org/10.1002/jat.3737.
27. Khetani SR, Szulgit G, Del Rio JA, Barlow C, Bhatia SN. Exploring interactions between rat hepatocytes and nonparenchymal cells using gene expression profiling. Hepatology. 2004;40(3):545–54. https://doi.org/10.1002/hep.20351.
28. Takayama K, Kawabata K, Nagamoto Y, Kishimoto K, Tashiro K, Sakurai F, Tachibana M, Kanda K, Hayakawa T, Furue MK. 3D spheroid culture of hESC/hiPSC-derived hepatocyte-like cells for drug toxicity testing. Biomaterials. 2013;34(7):1781–9. https://doi.org/10.1016/j.biomaterials.2012.11.029.
29. LeCluyse EL. Human hepatocyte culture systems for the in vitro evaluation of cytochrome P450 expression and regulation. Eur J Pharm Sci. 2001;13(4):343–68. https://doi.org/10.1016/s0928-0987(01)00135-x.
30. Li AP. Human hepatocytes: isolation, cryopreservation and applications in drug development. Chem Biol Interact. 2007;168(1):16–29. https://doi.org/10.1016/j.cbi.2007.01.001.
31. Godoy P, Hewitt NJ, Albrecht U, Andersen ME, Ansari N, Bhattacharya S, Bode JG, Bolleyn J, Borner C, Bottger J, Braeuning A, Budinsky RA, Burkhardt B, Cameron NR, Camussi G, Cho CS, Choi YJ, Craig Rowlands J, Dahmen U, . . . Hengstler JG. Recent advances in 2D and 3D in vitro systems using primary hepatocytes, alternative hepatocyte sources and non-parenchymal liver cells and their use in investigating mechanisms of hepatotoxicity, cell signaling and ADME. Arch Toxicol. 2013;87(8):1315-1530. https://doi.org/10.1007/s00204-013-1078-5
32. Prodanov L, Jindal R, Bale SS, Hegde M, McCarty WJ, Golberg I, Bhushan A, Yarmush ML, Usta OB. Long-term maintenance of a microfluidic 3D human liver sinusoid. Biotechnol Bioeng. 2016;113(1):241–6. https://doi.org/10.1002/bit.25700.
33. Davidson MD, Kukla DA, Khetani SR. Microengineered cultures containing human hepatic stellate cells and hepatocytes for drug development. Integr Biol (Camb). 2017;9(8):662–77. https://doi.org/10.1039/c7ib00027h.
34. Nguyen TV, Ukairo O, Khetani SR, McVay M, Kanchagar C, Seghezzi W, Ayanoglu G, Irrechukwu O, Evers R. Establishment of a hepatocyte-Kupffer cell coculture model for assessment of proinflammatory cytokine effects on metabolizing enzymes and drug transporters. Drug Metab Dispos. 2015;43(5):774–85. https://doi.org/10.1124/dmd.114.061317.
35. Ware BR, Durham MJ, Monckton CP, Khetani SR. A cell culture platform to maintain long-term phenotype of primary human hepatocytes and endothelial cells. Cell Mol Gastroenterol Hepatol. 2018;5(3):187–207. https://doi.org/10.1016/j.jcmgh.2017.11.007.
36. Khetani SR, Chen AA, Ranscht B, Bhatia SN. T-cadherin modulates hepatocyte functions in vitro. FASEB J. 2008;22(11):3768–75. https://doi.org/10.1096/fj.07-105155.
37. Kane BJ, Zinner MJ, Yarmush ML, Toner M. Liver-specific functional studies in a microfluidic array of primary mammalian hepatocytes. Anal Chem. 2006;78(13):4291–8. https://doi.org/10.1021/ac051856v.
38. Ranucci CS, Kumar A, Batra SP, Moghe PV. Control of hepatocyte function on collagen foams: sizing matrix pores toward selective induction of 2-D and 3-D cellular morphogenesis. Biomaterials. 2000;21(8):783–93. https://doi.org/10.1016/S0142-9612(99)00238-0.
39. McCuskey RS. Anatomy of the liver. Zakim and Boyer's hepatology. 5th ed. A textbook of liver disease. 2012;3–21. https://doi.org/10.1016/B978-1-4160-3258-8.50006-1.
40. Allen JW, Bhatia SN. Formation of steady-state oxygen gradients in vitro: application to liver zonation. Biotechnol Bioeng. 2003;82(3):253–62. https://doi.org/10.1002/bit.10569.
41. Kietzmann T, Freimann S, Bratke J, Jungermann K. Regulation of the gluconeogenic phosphoenolpyruvate carboxykinase and the glycolytic aldolase A gene expression by O2 in rat hepatocyte cultures Involvement of hydrogen peroxide as mediator in the response to O2. FEBS Lett. 1996;388(2–3):228–32. https://doi.org/10.1016/0014-5793(96)00557-1.
42. Tanaka Y, Yamato M, Okano T, Kitamori T, Sato K. Evaluation of effects of shear stress on hepatocytes by a microchip-based system. Meas Sci Technol. 2006;17(12):3167. https://doi.org/10.1088/0957-0233/17/12/S08.
43. Duthie SJ, Collins AR. The influence of cell growth, detoxifying enzymes and DNA repair on hydrogen peroxide-mediated DNA damage (measured using the comet assay) in human cells. Free Radical Biol Med. 1997;22(4):717–24. https://doi.org/10.1016/S0891-5849(96)00421-2.
44. Gomez-Lechon M, Donato M, Lahoz A, Castell J. Cell lines: a tool for in vitro drug metabolism studies. Curr Drug Metab. 2008;9(1):1–11. https://doi.org/10.2174/138920008783331086.
45. Gómez-Lechón MJ, Tolosa L, Conde I, Donato MT. Competency of different cell models to predict human hepatotoxic drugs. Expert Opin Drug Metab Toxicol. 2014;10(11):1553–68. https://doi.org/10.1517/17425255.2014.967680.
46. McDonnell AM, Dang CH. Basic review of the cytochrome p450 system. J Adv Pract Oncol. 2013;4(4):263. https://doi.org/10.6004/jadpro.2013.4.4.7.
47. Shamay A, Homans R, Fuerman Y, Levin I, Barash H, Silanikove N, Mabjeesh S. Expression of albumin in nonhepatic tissues and its synthesis by the bovine mammary gland. J Dairy Sci. 2005;88(2):569–76. https://doi.org/10.3168/jds.S0022-0302(05)72719-3.
48. Bachetti T, Comini L, Francolini G, Bastianon D, Valetti B, Cadei M, Grigolato P, Suzuki H, Finazzi D, Albertini A. Arginase pathway in human endothelial cells in pathophysiological conditions. J Mol Cell Cardiol. 2004;37(2):515–23. https://doi.org/10.1016/j.yjmcc.2004.05.004.
49. Zhou X, Liu D, You L, Wang L. Quantifying fluid shear stress in a rocking culture dish. J Biomech. 2010;43(8):1598–602. https://doi.org/10.1016/j.jbiomech.2009.12.028.

50. Du Y, Li N, Yang H, Luo C, Gong Y, Tong C, Gao Y, Lu S, Long M. Mimicking liver sinusoidal structures and functions using a 3D-configured microfluidic chip. Lab Chip. 2017;17(5):782–94. https://doi.org/10.1039/c6lc01374k.
51. Evans DW, Moran EC, Baptista PM, Soker S, Sparks JL. Scale-dependent mechanical properties of native and decellularized liver tissue. Biomech Model Mechanobiol. 2013;12(3):569–80. https://doi.org/10.1007/s10237-012-0426-3.
52. Kim L, Toh YC, Voldman J, Yu H. A practical guide to microfluidic perfusion culture of adherent mammalian cells. Lab Chip. 2007;7(6):681–94. https://doi.org/10.1039/b704602b.
53. Wang Y, Lee D, Zhang L, Jeon H, Mendoza-Elias JE, Harvat TA, Hassan SZ, Zhou A, Eddington DT, Oberholzer J. Systematic prevention of bubble formation and accumulation for long-term culture of pancreatic islet cells in microfluidic device. Biomed Microdevices. 2012;14(2):419–26. https://doi.org/10.1007/s10544-011-9618-3.